Article

Discovery Medicine 2023; 35(176): 264–274
https://doi.org/10.24976/Discov.Med.202335176.27

Amonafide Induces HUVEC Senescence by Inhibiting Autophagy

Jing Xia[1,2,†], Yu Zhou[3,†], Siyue He[1,2], Manoj Kumar Vashisth[1,2], Huijie Jia[1,2], Qianlong Dai[1,2], Yufen He[4,*], Xiaobo Wang[1,2,*]

[1]Department of Human Anatomy Histology and Embryology, School of Basic Medicine, Dali University, 671000 Dali, Yunnan, China
[2]Key Laboratory of University Cell Biology Yunnan Province, 671000 Dali, Yunnan, China
[3]Department of Oncology, Du Jiang Yan Medical Center, 611800 Chengdu, Sichuan, China
[4]Department of Oncology, Jiang'an County Traditional Chinese Medicine Hospital, 644200 Yi Bin, Sichuan, China
*Correspondence: wxb4320062@163.com (Xiaobo Wang); H937555233@126.com (Yufen He)
[†]These authors contributed equally.
Published: 2 June 2023

Background: Amonafide (Amo), due to hematotoxicity and digestive tract symptoms, the clinical application of which is limited. Several studies have reported that chemotherapy side effects are closely related to cellular senescence accumulation. Our study aims to examine whether amonafide causes senescence in human umbilical vein endothelial cell (HUVEC) lines and investigate its mechanisms associated with senescence.

Methods: The experiments of expression of genes and proteins associated with aging were carried out with HUVEC cell lines. The experiments were divided into a control group and an amonafide group with different days. The HUVEC senescence cells were detected by SA-β-Gal staining, Western blotting detected the protein levels of p16, p53, AMPK (Adenosine 5'-Monophosphate (AMP)-Activated Protein Kinase), mTOR (mechanistic Target of Rapamycin), p62, and LC3 (microtubule-associated protein1 light chain 3, MAP1LC3). Fluorescence detected the expression of mRFP (monomeric Red Fluorescent Protein)-GFP (Green Fluorescent Protein)-LC3 and LC3 puncta of HUVEC cells. RT-qPCR (Real-Time Quantitative Polymerase Chain Reaction) tested the expressions of *p53*, *p21*, *IL* (Interleukin)-*1*β, *IL-6* (Interleukin-6), *IL-8* (Interleukin-8), and *MCP-1* (Monocyte Chemoattractant Protein-1). CCK-8 (Cell Counting Kit-8) assessed the HUVEC cell viability.

Results: Here, we reported that amonafide resulted in an increased proportion of SA-β-Gal positive cells, high expression of aging-related proteins (p53 $p < 0.05$; p16 $p < 0.05$), and aging-related genes (*p53* $p < 0.05$; *p21* $p < 0.05$; *IL-1*β $p < 0.05$; *IL-6* $p < 0.05$; *IL-8* $p < 0.05$; *MCP-1* $p < 0.05$) on the 3rd day. Mechanistically, amonafide could cause an increase in the levels of the mTOR ($p < 0.05$) on days 1 and 3, and p62 protein ($p < 0.05$) on day 1, and a decline in LC3II (microtubule-associated protein1 light chain 3II)/LC3I levels ($p < 0.05$) on day 3, which is associated with the regulation of senescence. Additionally, the viability of HUVECs (human umbilical vein endothelial cells) was significantly inhibited by amonafide starting with a concentration of 0.8 μm ($p < 0.05$).

Conclusions: We first discovered that amonafide caused normal cellular senescence in our experiments. Amonafide-induced cellular aging by inhibiting autophagy and activating the mTOR pathway. The findings may offer new strategies for managing adverse reactions to amonafide.

Keywords: amonafide; senescence; mTOR; autophagy

Introduction

Amonafide, a DNA intercalating agent, exhibits significant anticancer activities by interfering with topoisomerase 2 (Topo II) activity [1]. In recent years, many researchers have studied the chemotherapeutic effect of amonafide on tumors of various types, including melanoma, breast cancer, and hepatic carcinoma [2–4]. Amonafide was used in a Phase III clinical trial in secondary acute myeloid leukemia (SAML) [5]. Although amonafide has been used widely in the clinic forits powerful antitumor properties, it can cause serious side effects, including suppression of bone marrow (leukopenia, neutropenia, and anemia), phlebitis after chemotherapy and cardiac dysfunction, which limits its application [6]. Therefore, it is urgent to determine the reasons why adverse reactions occur.

Senescence is the permanent cell growth arrest in proliferating cells under different stresses. The morphological features of senescent cells include large, irregular cells with prominent nuclei and multiple nuclei [7]. Additionally, senescent cells release the SASP (Senescence-Associated Secretory Phenotype), which controls many of their non-cell-autonomous functions [8]. The aging process is characterized by a progressive decline in physiological func-

tion, increasing vulnerability to death [9]. The term 'aging' refers to the combination of diseases, disorders, and symptoms associated with old age, such as wrinkles and presbyopia, stroke, and cancer metastasis [10]. Chemotherapeutic drugs play a crucial role in cancer patients. The cytotoxicity of these drugs often causes a variety of similar side effects, such as immunosuppression, fatigue, anemia, nausea, diarrhea, and alopecia in dividing cells [11]. Scholars have recently found that chemotherapeutic drugs induce cellular changes such as senescence. Wu *et al*. [12] showed that doxorubicin-induced cardiotoxicity is associated with cardiomyocyte senescence. Demaria *et al*. [13] also reported that the senescence of cells is responsible for chemotherapy side effects and cancer relapse. Zheng *et al*. [14] stated that many antimetabolic drugs, including fluorouracil, treat malignant tumors by miscoding RNA and inhibiting DNA synthesis from promoting senescent endothelial cells. Endothelial senescence contributes to endothelial dysfunction and vascular diseases such as atherosclerosis, thus increasing cardiovascular risk [14]. Amonafide can prevent DNA strand religation, resulting in double-strand breaks (DSBs). DNA damage causes cellular aging [15]. Because of the mechanism of action of amonafide, we hypothesize that its side effects are related to inducing cellular senescence.

Autophagy is a process of cellular digestion that eliminates damaged macromolecules and organelles. Autophagy is closely related to aging. Under stress conditions such as chemotherapy, autophagy is altered in response to the adaptive cellular response, which is tightly controlled by signaling pathways modulating the cellular autophagic flux including mTOR (mechanistic Target of the Rapamycin) and AMPK (Adenosine 5'-Monophosphate (AMP)-Activated Protein Kinase). Dysregulated autophagy leads to the occurrence of senescence [16]. Several studies have shown that autophagy delays aging and life extension; However, autophagy inhibition leads to senescence [17].

The mTOR pathway is an evolutionarily conserved signaling pathway that integrates environmental and intracellular communication to coordinate the nutrients and regulation of autophagy in senescence [18]. Studies have also shown that multiple signal transduction pathways, including mTOR, modulate various aspects of autophagy, such as initiation, processing, and termination [19]. The activation of mTOR signaling downregulates autophagy and causes an accumulation of senescent cells [20]. Recently, researchers revealed that mTOR signaling plays an essential role in aging and age-related diseases [21]. In our current study, we examined the effects and mechanism of amonafide on HUVEC (human umbilical vein endothelial cell) lines and deeply explored the relationships between amonafide, senescence, the mTOR signaling pathway, and autophagy. This was the first time we found that amonafide caused HUVEC senescence by activating mTOR and inhibiting autophagy.

Materials and Methods

Materials

Amonafide (S1367), rapamycin (S1309), chloroquine diphosphate salt (CQ, S4157), and doxorubicin (S1208) were purchased from Selleck (Shanghai, China). L-glutamine (G0201), penicillin (S4610) and streptomycin (S2572) were purchased from Solarbio (Beijing, China). Adding a complete medium was considered a vehicle control.

Cell Culture

HUVECs were obtained from the Hunan Fenghui Biotechnology Co., Ltd. (Loudi, China). The cells had been tested for mycoplasma and validated by STR (Short Tandem Repeat). In Roswell Park Memorial Institute-1640 medium (RPMI-1640) supplemented with 10% fetal calf serum (FBS), the cells were cultured on gelatin at 37 °C with 5% CO_2. Cells in passages 3 to 5 were used in experiments. In 12-well cell culture plates, HUVECs were plated at a density of 3000 cells/cm^2 and grown until 70% confluency.

SA-β-Gal Staining

HUVECs were treated with amonafide and doxorubicin for five days. To observe the proportion of cellular senescence, we utilized a histochemical staining kit of cellular SA-β-Gal (Cat#G1580, Solarbio, Beijing, China) to detect cellular senescence according to the manufacturer's protocol. Blue-green staining of senescent cells was evident under an inverted microscope. The experiment was conducted three times.

Cell Viability Assays

Cell viability was detected by CCK-8 (Cell Counting Kit-8) reagent (CA1210, Solarbio, Beijing, China) following the recommendations provided by the manufacturer. HUVECs (1×10^4/well) were seeded into 96-well plates. All experiments were conducted in triplicate. Every well was seeded withcells suspended in 100 μL of complete medium with each treatment. After treatment, CCK-8 (10 μL/well) was added for an additional 2 h of incubation, and absorption was measured at 450 nm.

RNA Isolation and Real-Time qPCR (Quantitative Polymerase Chain Reaction) (RT-qPCR)

After treatment, HUVECs were lysed with Invitrogen TRIzol reagent (15596026CN, Thermo Scientific, Shanghai, China), and total RNA was extracted. The concentration of RNA was determined by an ultraviolet spectrophotometer (912A1024, NanoDrop, Thermo Scientific, Shanghai, China). The RNA concentration measured is measured in ng/μL. cDNA (complementary DNA) was synthesized utilizing M-MLV (Moloney Murine Leukemia Virus Reverse Transcriptase) reverse transcriptase (M5301,

Table 1. Primer sequences.

Primer name	Forward (5′→3′)	Reverse (5′→3′)
18s	TTGACGGAAGGGCACCACCAG	GCACCACCACCCACGGAATCG
h-p21	TGTCCGTCAGAACCCATGC	AAAGTCGAAGTTCCATCGCTC
h-p53	TGCGTGTGGAGTATTTGGATG	TGGTACAGTCAGAGCCAACCTC
h-IL-8	TTTTGCCAAGGAGTGCTAAAGA	AACCCTCTGCACCCAGTTTTC
h-IL-1β	CAGCCAGATGCAATCAATGCC	TGGAATCCTGAACCCACTTCT
h-MCP-1	ATGATGGCTTATTACAGTGGCAA	GTCGGAGATTCGTAGCTGGA
IL-6	ACTCACCTCTTCAGAACGAAT	CCATCTTTGGAAGGTTCAGGTTG

Promega, Madison, WI, USA) from 1 μg total RNA. The synthesized cDNA was subjected to PCR-based amplification. There was no genomic DNA in the samples. We used the HiScript II 1st Strand cDNA Synthesis kit instructions (R211-01, Vazyme, Nanjing, China), to amplify the synthesized cDNA on an ABI 7500 Fast Real-time PCR system (4359284, 7500Fast, Applied Biosystems, Carlsbad, CA, USA); The reverse transcription condition: 50 °C 15 min $\rightarrow$ 85 °C 5 sec. The primers for qRT-PCR were as follows (Table 1). Next, we used a Real-time fluorescence quantitative PCR instrument (7900, ABI, Waltham, MA, USA), followed by the instruction procedure for Real-time-PCR reaction using 2$\times$ SYBR (Synergy Brands) Green qPCR Master Mix (Q712-02, Vazyme, Nanjing, China), the experiment was repeated thrice using the 18 sec ribosomal RNA sequences as an internal reference.

The data were analyzed using Step One Software (v2.2, ABI, Waltham, MA, USA) to obtain the relative expression of genes. Using the $2^{-\Delta\Delta Ct}$ method to calculate each gene expression associated with the 18 sec.

Western Blot

Mammalian cell-PE LB^{TM} (polyethylene Lysis Buffer$^{Trade\ Marrk}$) buffer (Organic buffer & 10 Mm NaCl & detergent, Ph 7.5) (GB-180, G-Biosciences & Geno Technology, St. Louis, MO, USA) containing phosphatase (Sigma-Aldrich, St, Louis, MO, USA) was utilized to extract total proteins from harvested cells. All protein concentrations were detected using a BCA (Butyleyanoacrylate) protein assay kit (71285-M, Sigma-Aldrich, St. Louis, MO, USA). Protein samples for western blotting were separated by SDS-PAGE (Sodium Dodecyl Sulfate-Polyacrylamide Gel Electrophoresis) and transferred to polyvinylidene difluoride membranes (1620177, Bio-Rad, Hercules, CA, USA). The membrane was embedded with 5% skim milk for 1 h and then incubated with a primary antibody against GAPDH (glyceraldehyde-3-phosphate dehydrogenase) (1:2000 in 5% BSA (Bovine Serum Albumin)), (#5174, CST (Cell Signaling Technology, Inc.), Boston, MA, USA), p16 (1:1000, SR34-02, Huaan Biotechnology, Hangzhou, China), p53 (p6374, 1:1000, Invitrogen, Carlsbad, CA, USA), t-mTOR (Cat#2972, 1:1000, CST, Boston, MA, USA), p-mTOR (Cat#5536, 1:1000, CST, Boston, MA, USA), t-AMPK (Cat#5759, 1:1000, CST, Boston, MA, USA), p-AMPKα (Thr172) (Cat#2535, 1:1000, CST, Boston, MA, USA), p62 (Cat#48768, 1:1000, CST, Boston, MA, USA) and anti-LC3 (antibody recognizes LC3 (microtubule-associated protein 1 light chain 3, MAP1LC3)) (12741, 1:1000, CST, Boston, MA, USA) followed by incubation with a Peroxidase-conjugated secondary antibody for 1 h at room temperature. Peroxidase-conjugated Affinipure Goat anti-Mouse IgG (immunoglobulin G) (H + L) (Cat#SA00001-1, 1:10000) was from Proteintech (Wuhan, China). Peroxidase-conjugated Affinipure Goat anti-Rabbit IgG (H + L) (Cat#SA00001-2, 1:10000) was from Proteintech (Wuhan, China). The western blot grayscale value was measured with the ImageJ (V1.8.0.112, National Institutes of Health, Bethesda, MD, USA) software. Final grey value = (target gene band grey value – blank value)/(reference gene band grey value – blank value), n = 3.

Fluorescence Analysis of Cells Expressing mRFP (monomeric Red Fluorescent Protein)-GFP (Green Fluorescent Protein)-LC3 and LC3 Puncta

According to the manufacturer's instructions, the mRFP-GFP-LC3 plasmid (gt-ap-p101, Xingtuo Biotechnology, Shanghai, China) was cotransfected into HUVECs, and G418 sulfate (108321-42-2, Solbio, Beijing, China) was added. In these cells, red fluorescent protein (RFP) and green fluorescent protein (GFP) fluorescence was used to investigate the intracellular localization of LC3 protein. We obtained images on an inverted fluorescence microscope. By applying the colocalization macro for red and green puncta to the red and green colocalization macro puncta for the ImageJ program, we determined the number of puncta of LC3 [21]. LC3 puncta were counted in 40 randomly chosen cells per treatment group. The GFP+RFP+ puncta have a yellow color, and the GFP–RFP+ puncta have a red color. The experiment was conducted three times.

Statistical Analysis

GraphPad Prism (Version 6.0, GraphPad Software Inc., San Diego, CA, USA) was used for statistical data analysis. All data are expressed as the mean $\pm$ SD (Standard Deviation). Among multiple groups, one-way ANOVA (Analysis of Variance) was performed. Intergroup differences were analyzed by using Tukey's test. p values

< 0.05 were deemed statistically significant. An assay was performed in triplicate.

Results

Amonafide Activates SA-β-Gal Activity in HUVECs and Inhibits Cell Viability

Regarding cellular senescence, we examined the effect of amonafide on HUVECs. Researchers have reported that doxorubicin may lead to normal cellular senescence [12]. HUVECs are frequently used to build cellular senescence models. As shown in Fig. 1a,b, when HUVECs were exposed to amonafide at concentrations between 0.3 μm and 1.0 μm, more were stained blue-green by SA-β-Gal than the control group. Furthermore, we discovered that the ratio of positive cells was over 40% within the range of Amo-treated concentrations (0.3–1.0 μm), especially with concentrations of 0.5 μm, the positive ratio of which was similar to that of doxorubicin (0.15 μm) (Fig. 1a,c, $p < 0.05$). Based on these data, amonafide, similar to doxorubicin, could induce cells to enter a senescent state. Amo-treated HUVECs became large and flattened as the days passed, and on day 4, dead cells began to appear (Fig. 1d,e, $p < 0.05$). We then determined the viability of cells at different concentrations. The viability test was performed after HUVECs were treated with amonafide for 3 days. As shown in Fig. 1f, cell viability declined rapidly from 0.8 μm amonafide ($p < 0.01$). The above result demonstrates that cell viability is not only affected by amonafide in a dose-dependent manner, but amonafide also leads to cellular senescence.

Amonafide can Induce an Increase in Aging-Related Proteins and the Production of SASP in HUVECs

Cellular senescence is a stress response that induces irreversible cell cycle halt and substantial phenotypic alterations, including the formation of a bioactive secretome, known as SASP. In cellular senescence, accompanied by the increase of p53 and p16 protein levels and the activation of the senescence-related level of mRNA (messenger Ribonucleic Acid) of *p53*, *p21* [15]. The study found a gradual increase in p16 and p53 protein levels from day 1 to day 3 (Fig. 2a–c, $p < 0.05$). *p53* and *p21* mRNA expression gradually increased from day 1 to day 3 (Fig. 2d,e, $p < 0.05$). Consistent with the above results, SASP, such as *IL-1β* (Interleukin-1β), *IL-6* (Interleukin-6), *IL-8* (Interleukin-8), and *MCP-1* (Monocyte Chemoattractant Protein-1), were significantly increased on day 3 (Fig. 2f–i, $p < 0.05$). According to these data, amonafide activates aging-related secretion phenotypes and drives the expression of aging markers in HUVECs.

Amonafide Causes Cellular Aging by Interfering with Autophagy

Autophagy is closely linked to aging; Researchers have demonstrated that hindering autophagy should result in senescence. To illustrate the relationship between autophagy and amonafide-induced HUVEC senescence, we used three detection methods: Western blotting, SA-β-Gal staining, and immunofluorescence. Autophagy is closely associated with the expression levels of proteins including LC3 and p62 [22,23]. The LC3II (microtubule-associated protein1 light chain 3II)/LC3I ratio decreases when autophagy is suppressed as p62 protein levels rise. As shown in Fig. 3a–c, when HUVECs were treated with amonafide from 1 to 3 days, the p62 protein level statistically significantly increased on day 1 and was slightly elevated on day 3 ($p < 0.05$). Autophagy flux refers to the sum of autophagic molecular events, ranging from autophagy induction and autophagosome formation to autolysosomal degradation and lysosome reformation [24]. LC3 is commonly considered a model substrate to measure autophagic flux. HUVECs were stably transfected with an RFP-GFP-LC3 protein in tandem to detect LC3, followed by GFP+RFP+ appearing yellow and GFP–RFP+ appearing red [25]. Yellow LC3 puncta indicate nonfunctional autolysosomes and inactive autophagic flux, whereas red LC3 puncta represent the opposite result (Fig. 3d). The immunofluorescence results showed that under oxidative stress induced by amonafide, the red LC3 dots of LC3 punctate cells of HUVECs gradually decreased, while the yellow LC3 dots increased (Fig. 3e,f). Chloroquine diphosphate salt (CQ), an inhibitor of lysosomes, is used to perform blocking experimental proofs. Compared to the control group, the CQ group showed higher levels of p62 expression and lower levels of LC3II/LC3I. However, the addition of CQ did not result in a higher level of p62 and a lower ratio of LC3II/LC3I expression of these molecules compared to the amonafide treatment group (Fig. 3g–i, $p < 0.05$). According to Fig. 3j,k, CQ did not increase the yellow LC3 puncta over a broader range, indicating that the CQ and amonafide groups all had low degradation potency. Additionally, senescent cells were increased with the addition of CQ alone, consistent with the SA-β-Gal staining ratio of the amonafide treatment group alone. The two reagent combinations did not result in a further increase in senescence cells. These findings indicate that amonafide induces senescence in cells by inhibiting autophagy.

Autophagy and Autophagy Flux are Inhibited by Amonafide through the mTOR Pathway

Both AMPK and mTOR are major junctions in the autophagy-regulating signaling network [26]. Next, we investigated how autophagy is inhibited by monitoring these two critical signaling pathways. Proteins were harvested from HUVECs at 1 and 3 days after amonafide treatment, respectively, and western blotting was performed. On day

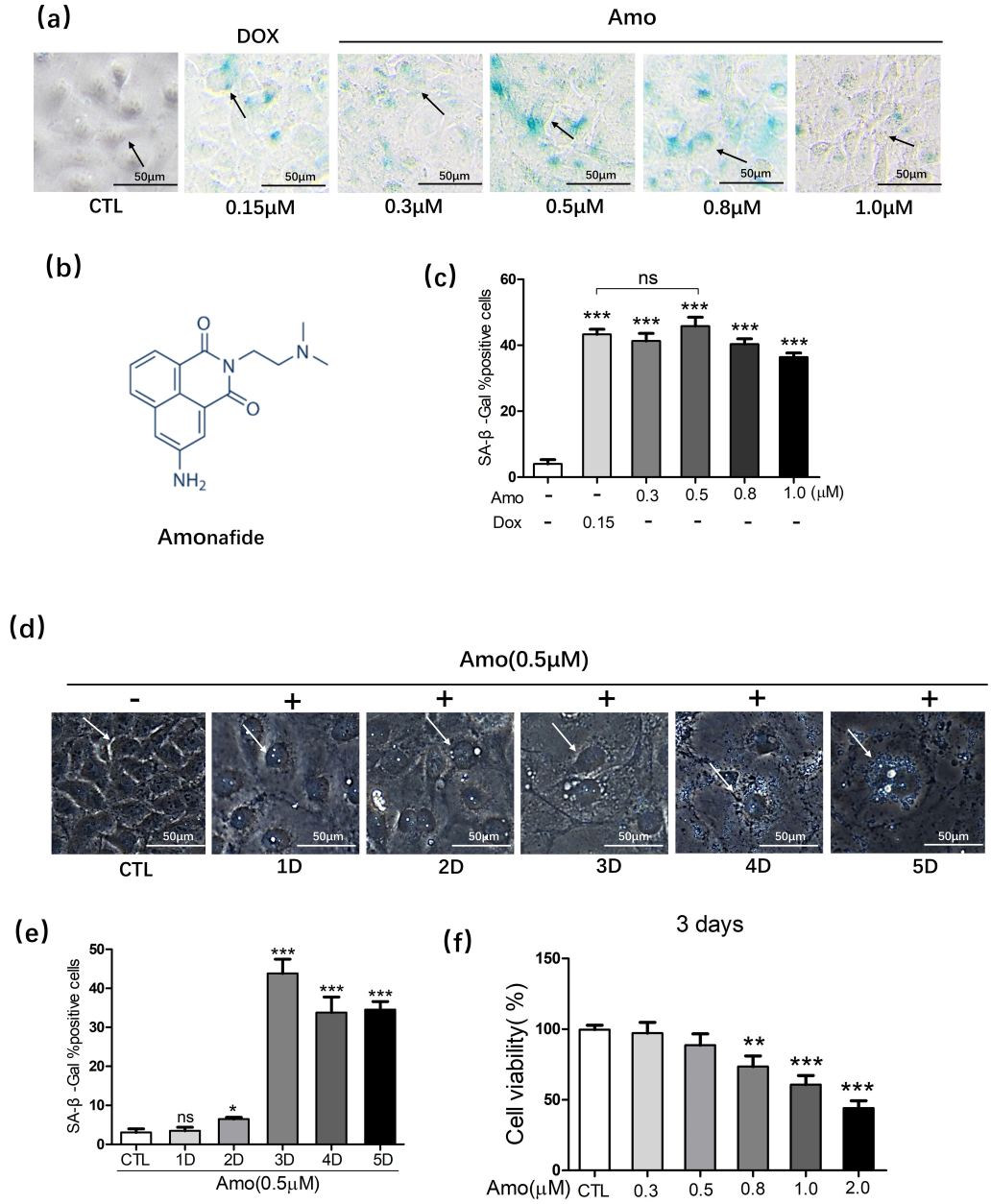

Fig. 1. Amonafide (Amo) treatment increases SA-β-Gal activity and reduces cell viability. (a) Representative images of HUVECs and SA-β-Gal staining after treatment with amonafide at concentrations from 0.3 to 1.0 μm for 3 days and 0.15 μm doxorubicin (Dox) as a positive control. Scale bars: 50 μm. (b) Molecular formula of amonafide. (c) Percentage of SA-β-Gal-stained senescent cells. (d) HUVECs treated with 0.5 μm amonafide from 0 to 5 days and the vehicle control. Scale bars: 50 μm. (e) The proportion of senescent HUVECs. (f) HUVEC viability after treatment with various concentrations of amonafide (0.3–2.0 μm) for three days. The results are presented as the means $\pm$ SD. n = 3. $^{*}p < 0.05$, $^{**}p < 0.01$, $^{***}p < 0.001$ compared to the control (CTL). "ns" is defined as not statistically significant. D, day. "–" represents no medicine; "+" represents the presence of medication.

3, mTOR phosphorylation levels increased significantly, whereas AMPK phosphorylation levels did not change significantly (Fig. 4a–c, $p < 0.05$). Next, we focused on the mTOR signaling pathway and conducted experiments to block it. Rapamycin, an mTOR-dependent autophagy activator, was chosen for inhibition experiments. As indicated in Fig. 4d,e, rapamycin inhibited the protein phosphorylation level of amonafide-activated mTOR in cells, especially on the 3rd day, when compared to the amonafide group. Furthermore, when rapamycin was added, autophagy associated with amonafide was reactivated. The results revealed a decrease in p62 protein levels and an increase in LC3II (microtubule-associated protein1 light chain 3II)/LC3I ratios (Fig. 4d,f,g, $p < 0.05$). According to immunofluorescence, the amonafide group had more yellow LC3 spots than rapamycin, while the rapamycin group had increased

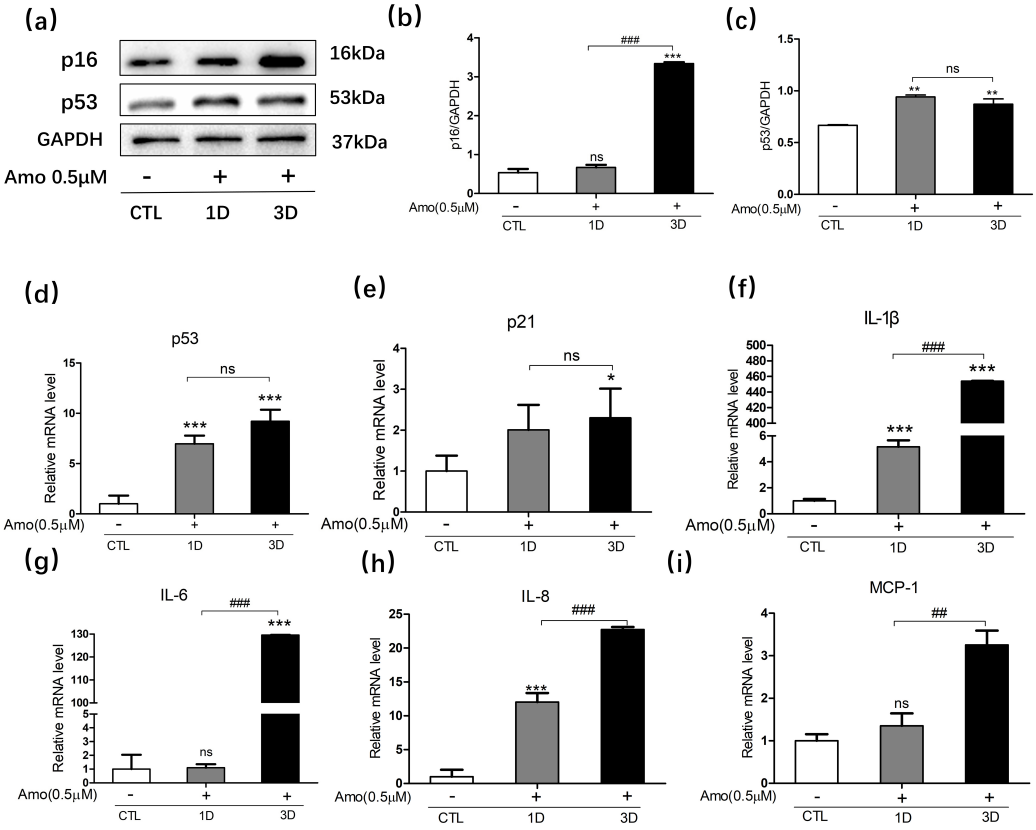

Fig. 2. Senescence-associated proteins and gene expression are increased in Amonafide (Amo)-treated HUVECs. (a) p16, p53 protein levels were examined on day 1 and day 3 after treatment with 0.5 μm amonafide. (b,c) Quantification of the relative protein levels. n = 3. (d–i) Relative RNA expression of *p53*, *p21*, *IL-1*β, *IL-6*,*IL-8*, and *MCP-1* was analyzed by qRT-PCR. The results are presented as the means $\pm$ SD. $^{*}p < 0.05$, $^{**}p < 0.01$, $^{***}p < 0.001$ compared to the control (CTL). $^{\#\#}p < 0.01$, $^{\#\#\#}p < 0.001$ compared to the indicated sample. "ns" is defined as not statistically significant. 1D, day 1; 3D, day 3. "–" represents no medicine; "+" represents the presence of medication.

red LC3 puncta (Fig. 4h,i). Meanwhile, the percentage of SA-β-Gal-positive cells significantly decreased in the amonafide plus rapamycin groups compared to the amonafide group (Fig. 4j,k, $p < 0.05$). Based on these results, amonafide limits autophagic flux and causes senescence in HUVECs by stimulating the mTOR pathway.

Discussion

In mammalian tissues, senescent cells increase with age and have been found at age-related pathological sites such as osteoarthritis and atherosclerosis [26,27], indicating that senescence plays a role in the aging of organisms. In addition, chemotherapy has been shown to induce cellular senescence in human patients [28]. Two recent studies have shown that the selective removal of senescent cells induced by chemotherapy ameliorates the adverse effects of chemotherapy and improves tissue homeostasis in mice [29–31]. Bhayadia *et al.* [32] point out that endothelial senescence might be induced by endothelial dysfunction. This study is the first to demonstrate that amonafide, one of the broad-spectrum antitumor drugs in clinical use, can cause human HUVECs to age and significantly suppresses the proliferation ability and activity of HUVECs. This discovery makes us understand the relationship between the side effects of amonafide and aging and provides a new theoretical basis for the clinical treatment of amonafide-related side effects. Furthermore, the experiments showed that amonafide inhibits autophagy and autophagy flux in cells by activating mTOR, not AMPK.

In recent years, researchers have investigated the efficacy of amonafide in treating blood-related diseases and solid malignancies, such as lung and breast cancer [2,5,33]. The side effects of chemotherapy drugs, such as suppression of bone marrow and cardiovascular injury, limit their use. In our study, we found that amonafide induced a decrease in cell viability, proinflammatory cytokine release (*IL-1*β, *TNF-*α, *IL-8*, *MCP-1*), and an increase in SA-β-Gal activity as well as aging-related proteins and genes (*p16, p53, p21*). These play an essential role in the application of amonafide in chemotherapy. Unfortunately, adverse reactions significantly limit its application. It is necessary

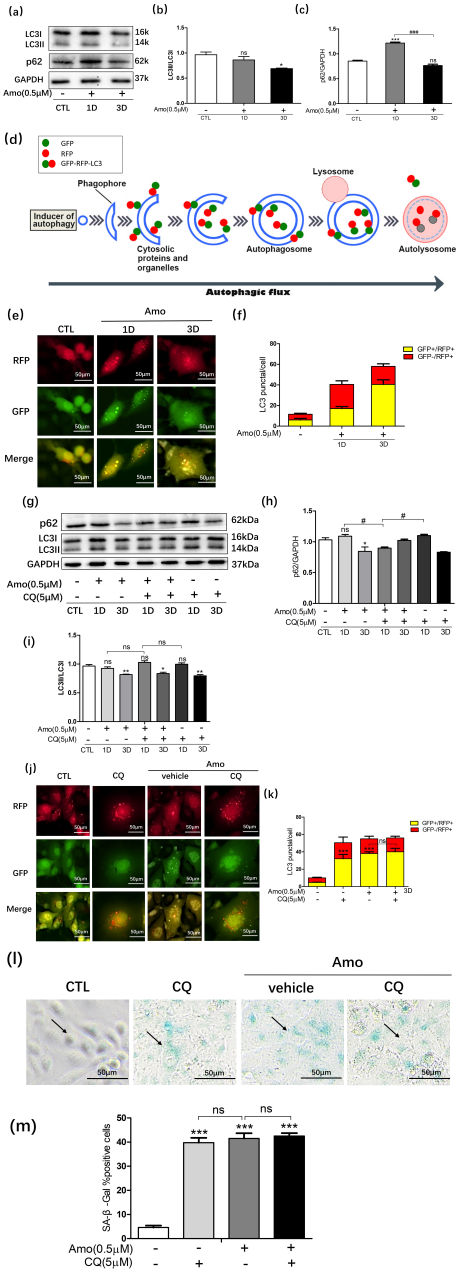

Fig. 3. Amonafide (Amo) inhibits autophagy, resulting in cellular senescence. (a) HUVECs treated with 0.5 μm amonafide from 1 to 3 days were measured for LC3-II, LC3-I, and p62 expression protein levels. (b,c) Quantification of relative protein levels based on three independent experiments. (d) The image of autophagy flow works of mGFP-RFP-LC3. In the overlapping picture, the dot-like aggregation is considered to be autophagosomes when it is yellow, and autophagic lysosomes when it is red. The patency of autophagy is evaluated by the ratio of yellow and red bright spots, that is, the state of autophagy flow. (e) GFP-RFP-LC3-expressing cells were incubated from 1 to 3 days with amonafide (0.5 μm) to observe GFP, RFP, and their overlapping images. (f) The average number of LC3 puncta in each cell is based on image (e), n = 3. (g) The protein levels of LC3-II, LC3-I, and p62 were measured in HUVECs treated with 0.5 μm amonafide, 5 μm chloroquine diphosphate salt (CQ) or the combination on days 1 and 3. (h,i) Quantification of relative protein levels. n = 3. (j,k) The fluorescence of cells expressing RFP-GFP-LC3 and the numbers of LC3 puncta on average per cell. n = 3. (l) Representative images of cells stained with SA-β-Gal. (m) The percentage of SA-β-Gal-positive cells in (l). The results are presented as the means $\pm$ SD, n = 3. $^{*}p < 0.05$, $^{***}p < 0.001$ compared to the control (CTL). $^{\#}p < 0.05$, $^{\#\#\#}p < 0.001$ compared to the indicated sample. “ns” is defined as not statistically significant. 1D, day 1; 3D, day 3. “–” represents no medicine; “+” represents the presence of medication.

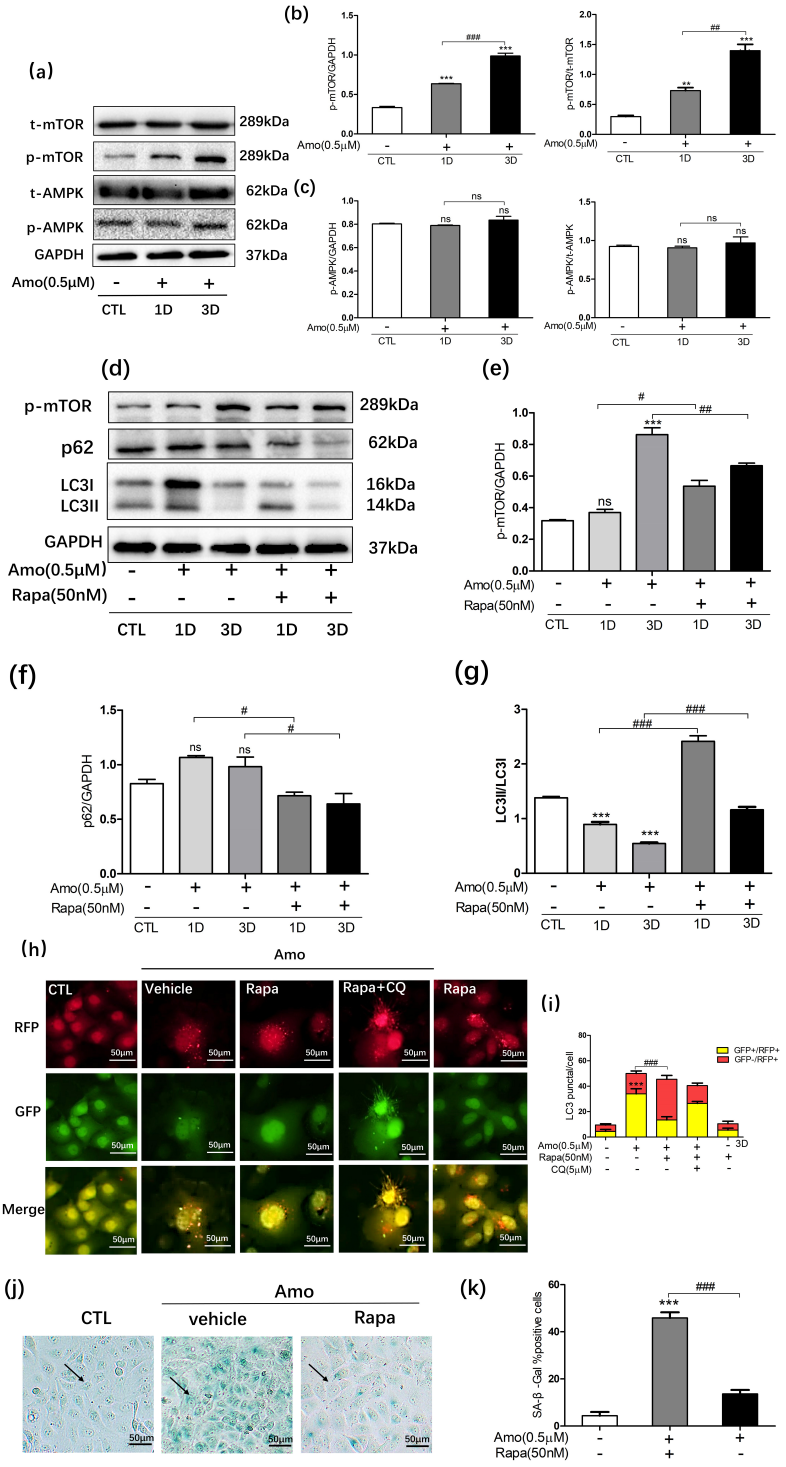

Fig. 4. Amonafide (Amo) suppresses autophagy and autophagy flux by activating the mTOR signaling pathway. (a) Protein expression levels of t-mTOR, p-mTOR, t-AMPK, and p-AMPK in HUVECs treated with and without amonafide on days 1 and 3. (b,c) Quantification of relative protein levels. n = 3. (d) Protein levels of t-mTOR, p-mTOR, p62, LC3-II, and LC3-I in HUVECs treated with 0.5 μm amonafide alone or amonafide plus 50 nm rapamycin on days 1 and 3. (e–g) Quantification of relative protein levels. n = 3. (h,i). The fluorescence images of cells expressing RFP-GFP-LC3 and the amounts of LC3 puncta on average per cell. n = 3. (j) Representative images of SA-β-Gal staining of cells. (k) Percentage of SA-β-Gal-positive cells based on images presented in (j). The results are presented as the means ± SD. n = 3. $^{**}p < 0.01$, $^{***}p < 0.001$ compared to the control (CTL). $^{\#}p < 0.05$, $^{\#\#}p < 0.01$, $^{\#\#\#}p < 0.001$ compared to the indicated sample. "ns" is defined as not statistically significant. 1D, day 1; 3D, day 3. "–" represents no medicine; "+" represents the presence of medication.

to look for possible mechanisms causing adverse reactions. The above data show that amonafide significantly induced cellular senescence in HUVECs, which might be closely linked with the side effects. The research supplies new thoughts for the in-depth study of amonafide.

Chemotherapeutic agents, such as doxorubicin, fluorouracil, and amonafide, are common for patients with advanced cancer. However, patients frequently suffer and experience systemic toxicity and many adverse outcomes from treatment, including weight and hair loss, vomiting, and an increased risk of infection. Research has increasingly focused on TIS (Therapeutic Induced Senescence), which may become a new target for relieving adverse chemotherapy effects. In addition to adverse effects, the cause of recurrence after a period of chemotherapy treatment is also a problem we need to address. In recent years, researchers have found that TIS leads to adverse side effects and may activate cancer cells' invasive properties and induce stemness, simultaneously increasing the risk of tumor recurrence [34]. Our research only studied the relationship between amonafide and normal cells; We will also focus on the relationship between amonafide and cancer cell resistance.

Recent research has found that autophagy is a dynamic process that allows endothelial cells (ECs) to respond to environmental changes and regulate their function [35]. The age-related inhibition of proteostasis and consequent accumulation of protein aggregates in ECs have been associated with defects in autophagy and endothelial dysfunction. A possible mechanism between autophagy and senescence is that inhibition of autophagy can regulate the activation of the SASP [36]. A well-known function of p62 is to induce SASP production and activate the mTOR pathway through amino acid sensing. As a result of increased levels of p62 in autophagy-deficient cells, proteasomal degradation is inhibited, leading to the accumulation of protein aggregates.

In the present research, we found that autophagy-related proteins and p62 protein levels were upregulated, and LC3I and LC3II protein levels were considerably altered. Amonafide induced cellular aging of endothelial cells by activating the senescence critical node mTOR signaling pathway and inhibiting autophagy. The activation of mTOR was closely linked with the adverse effects of amonafide. These new findings establish a theoretical foundation for evaluating the toxicological impacts of amonafide *in vitro*. Perhaps the choice of an mTOR-dependent autophagy activator would be an option for the remission of the side effects of amonafide.

Rapamycin is a known anti-aging drug used as an antiproliferative and immunosuppressive drug with a variety of clinical applications [37]. *In vitro* experiments have indicated that rapamycin can alleviate senescence induced by amonafide. We will conduct animal experiments in the future to further study the mitigating effects of rapamycin. In a study by Feng *et al.* [38], aspirin's effects on doxorubicin's late-onset side effects were ameliorated by senescence suppression. Aljobaily *et al.* [39] also found that creatine protects the liver from doxorubicin-induced damage by preventing cellular senescence. Related research based on similarity and anti-aging drugs may play a crucial role in mitigating the negative impact of amonafide. Further studies will look at anti-aging medications and examine whether anti-aging treatments might mitigate the adverse effects of amonafide.

Conclusions

Amonafide was studied for its effect on cellular senescence. We have clarified the mechanisms that cause HUVECs to senescence by inhibiting autophagy through impaired autophagy flux and activating the mTOR signaling pathway. The findings may provide new strategies for the clinical management of adverse reactions to amonafide.

Abbreviations

Amo, Amonafide; AMPK, AMP-Activated Protein Kinase; CTL, Control; DSBs, Double-Strand Breaks; Dox, Doxorubicin; ECs, Endothelial Cells; GFP, Green Fluorescent Protein; HUVEC, Human Umbilical Vein Endothelial Cell; *IL-1β*, Interleukin-1β; *IL-6*, Interleukin-6; *IL-8*, Interleukin-8; *MCP-1*, Monocyte Chemoattractant Protein–1; mTOR, mammalian Target of Rapamycin; RFP, Red Fluorescent Protein; SAML, Secondary Acute Myeloid Leukemia; SASP, Senescence-Associated Secretory Phenotype; Topo II, Topoisomerase 2.

Author Contributions

JX, YFH, and XBW—designed the research study; JX and YZ—performed the research; JX, MKV, HJJ, SYH, QLD, and YFH—provided help and advice on western blotting, qPCR, immunohistochemistry, and other experiments; MKV, HJJ, YZ, SYH, and QLD—analyzed the data. All authors contributed to editorial changes in the manuscript. All authors read and approved the final manuscript. All authors have participated sufficiently in the work and agreed to be accountable for all aspects of the work.

Ethics Approval and Consent to Participate

Not applicable.

Acknowledgment

Not applicable.

Funding

This work was funded by The China National Natural Science Foundation (Grant No. 81860158) and Le Shan City Key Research Project (Grant No. 19SZD188) (Grant No. 19SZD212).

Conflict of Interest

The authors declare no conflict of interest.

References

[1] Walunj D, Thankarajan E, Prasad C, *et al*. Targeted methylation facilitates DNA double strand breaks and enhances cancer suppression: A DNA intercalating/methylating dual-action chimera Amonafidazene. *Eur J Med Chem*. 2021;225:113811. doi: 10.1016/j.ejmech.2021.113811

[2] Ye Y, Huang S, Wu Y. UNBS5162 and amonafide inhibits tumor progression in human melanoma by the AKT/mTOR pathway. *Cancer Manag Res*. 2019;11:2339–2348. doi: 10.2147/CMAR.S177623

[3] Zhao J, Lu M, Lai H, *et al*. Delivery of Amonafide from Fructose-Coated Nanodiamonds by Oxime Ligation for the Treatment of Human Breast Cancer. *Biomacromolecules*. 2018;19(2):481–489. doi: 10.1021/acs.biomac.7b01592

[4] Ma J, Li L, Yue K, *et al*. A naphthalimide-polyamine conjugate preferentially accumulates in hepatic carcinoma metastases as a lysosome-targeted antimetastatic agent. *Eur J Med Chem*. 2021;221:113469. doi: 10.1016/j.ejmech.2021.113469

[5] Stone RM, Mazzola E, Neuberg D, *et al*. Phase III open-label randomized study of cytarabine in combination with amonafide L-malate or daunorubicin as induction therapy for patients with secondary acute myeloid leukemia. *J Clin Oncol*. 2015;33(11):1252–1257. doi: 10.1200/JCO.2014.57.0952

[6] Ma J, Li Y, Li L, *et al*. A Polyamine-Based Dinitro-Naphthalimide Conjugate as Substrates for Polyamine Transporters Preferentially Accumulates in Cancer Cells and Minimizes Side Effects *in vitro* and *in vivo*. *Front Chem.* 2020;8:166. doi: 10.3389/fchem.2020.00166

[7] Zhang H, Stallock JP, Ng JC, Reinhard C, Neufeld TP. Regulation of cellular growth by the Drosophila target of rapamycin dTOR. *Genes Dev*. 2000;14(21):2712–2724. doi: 10.1101/gad.835000

[8] Cianflone E, Torella M, Biamonte F, *et al*. Targeting Cardiac Stem Cell Senescence to Treat Cardiac Aging and Disease. *Cells*. 2020;9(6):1558. doi: 10.3390/cells9061558

[9] Blagosklonny MV. From rapalogs to anti-aging formula. *Oncotarget.* 2017;8(22):35492–35507. doi: 10.18632/oncotarget.18033

[10] Chen Z, Li C, Huang H, Shi YL, Wang X. Research progress of aging-related microRNAs. *Curr Stem Cell Res Ther*. 2023. doi: 10.2174/1574888X18666230308111043

[11] Schünemann M, Anker SD, Rauchhaus M. Cancer fatigue syndrome reflects clinically non-overt heart failure: an approach towards onco-cardiology. *Nat Clin Pract Oncol*. 2008;5(11):632–633. doi: 10.1038/ncponc1226

[12] Wu YZ, Zhang L, Wu ZX, Shan TT, Xiong C. Berberine Ameliorates Doxorubicin-Induced Cardiotoxicity via a SIRT1/p66Shc-Mediated Pathway. *Oxid Med Cell Longev*. 2019;2019:2150394. doi: 10.1155/2019/2150394

[13] Demaria M, O'Leary MN, Chang J, *et al*. Cellular Senescence Promotes Adverse Effects of Chemotherapy and Cancer Relapse. *Cancer Discov*. 2017;7(2):165–176. doi: 10.1158/2159-8290.CD-16-0241

[14] Zheng M, Chen Y, Park J, *et al*. CO ameliorates endothelial senescence induced by 5-fluorouracil through SIRT1 activation. *Arch Biochem Biophys*. 2019;677:108185. doi: 10.1016/j.abb.2019.108185

[15] Jia H, Vashisth MK, Ge Y, Dai Q, He F, Wang X. Anti-inflammation and anti-aging mechanisms of mercaptopurine *in vivo* and *in vitro*. *Biochem Biophys Res Commun*. 2023;638:103–111. doi: 10.1016/j.bbrc.2022.11.035

[16] Tang C, Livingston MJ, Liu Z, Dong Z. Autophagy in kidney homeostasis and disease. *Nat Rev Nephrol*. 2020;16(9):489–508. doi: 10.1038/s41581-020-0309-2

[17] Tai H, Wang Z, Gong H, *et al*. Autophagy impairment with lysosomal and mitochondrial dysfunction is an important characteristic of oxidative stress-induced senescence. *Autophagy*. 2017;13(1):99–113. doi: 10.1080/15548627.2016.1247143

[18] Weichhart T. mTOR as Regulator of Lifespan, Aging, and Cellular Senescence: A Mini-Review. *Gerontology*. 2018;64(2):127–134. doi: 10.1159/000484629

[19] Wang Y, Zhang H. Regulation of Autophagy by mTOR Signaling Pathway. *Adv Exp Med Biol*. 2019;1206:67–83. doi: 10.1007/978-981-15-0602-4_3

[20] Kim YC, Guan KL. mTOR: a pharmacologic target for autophagy regulation. *J Clin Invest*. 2015;125(1):25–32. doi: 10.1172/JCI73939

[21] Vellai T, Takacs-Vellai K, Zhang Y, Kovacs AL, Orosz L, Müller F. Genetics: influence of TOR kinase on lifespan in C. elegans. *Nature*. 2003;426(6967):620. doi: 10.1038/426620a

[22] Mizushima N, Yoshimori T, Levine B. Methods in mammalian autophagy research. *Cell*. 2010;140(3):313–326. doi: 10.1016/j.cell.2010.01.028

[23] Chi C, Li DJ, Jiang YJ, *et al*. Vascular smooth muscle cell senescence and age-related diseases: State of the art. *Biochim Biophys Acta Mol Basis Dis*. 2019;1865(7):1810–1821. doi: 10.1016/j.bbadis.2018.08.015

[24] Yoshii SR, Mizushima N. Monitoring and Measuring Autophagy. *Int J Mol Sci*. 2017;18(9):1865. doi: 10.3390/ijms18091865

[25] Klionsky DJ, Abdel-Aziz AK, Abdelfatah S, *et al*. Guidelines for the use and interpretation of assays for monitoring autophagy (4th edition)[1]. *Autophagy*. 2021;17(1):1–382. doi: 10.1080/15548627.2020.1797280

[26] Alers S, Löffler AS, Wesselborg S, Stork B. Role of AMPK-mTOR-Ulk1/2 in the regulation of autophagy: cross talk, shortcuts, and feedbacks. *Mol Cell Biol*. 2012;32(1):2–11. doi: 10.1128/MCB.06159-11

[27] Price JS, Waters JG, Darrah C, *et al*. The role of chondrocyte senescence in osteoarthritis. *Aging Cell*. 2002;1(1):57–65. doi: 10.1046/j.1474-9728.2002.00008.x

[28] Matthews C, Gorenne I, Scott S, *et al*. Vascular smooth muscle cells undergo telomere-based senescence in human atherosclerosis: effects of telomerase and oxidative stress. *Circ Res*. 2006;99(2):156–164. doi: 10.1161/01.RES.0000233315.38086.bc

[29] Sanoff HK, Deal AM, Krishnamurthy J, *et al*. Effect of cytotoxic chemotherapy on markers of molecular age in patients with breast cancer. *J Natl Cancer Inst*. 2014;106(4):dju057. doi: 10.1093/jnci/dju057

[30] Demaria M, O'Leary MN, Chang J, *et al*. Cellular Senescence Promotes Adverse Effects of Chemotherapy and Cancer Relapse. *Cancer Discov*. 2017;7(2):165–176. doi: 10.1158/2159-8290.CD-16-0241

[31] Baar MP, Brandt RMC, Putavet DA, *et al*. Targeted Apoptosis of Senescent Cells Restores Tissue Homeostasis in Response to Chemotoxicity and Aging. *Cell*. 2017;169(1):132–147.e16. doi: 10.1016/j.cell.2017.02.031

[32] Bhayadia R, Schmidt BM, Melk A, Hömme M. Senescence-Induced Oxidative Stress Causes Endothelial Dysfunction. *J Gerontol A Biol Sci Med Sci*. 2016;71(2):161–169. doi: 10.1093/gerona/glv008

[33] Gilad Y, Tuchinsky H, Ben-David G, *et al*. Discovery of potent molecular chimera (CM358) to treat human metastatic melanoma. *Eur J Med Chem*. 2017;138:602–615. doi: 10.1016/j.ejmech.2017.06.066

[34] Olszewska A, Borkowska A, Granica M, *et al*. Escape From

Cisplatin-Induced Senescence of Hypoxic Lung Cancer Cells Can be Overcome by Hydroxychloroquine. *Front Oncol*. 2022;11:738385. doi: 10.3389/fonc.2021.738385

[35] Mameli E, Martello A, Caporali A. Autophagy at the interface of endothelial cell homeostasis and vascular disease. *FEBS J*. 2022;289(11):2976–2991. doi: 10.1111/febs.15873

[36] Salazar G, Cullen A, Huang J, *et al*. SQSTM1/p62 and PPARGC1A/PGC-1alpha at the interface of autophagy and vascular senescence. *Autophagy*. 2020;16(6):1092–1110. doi: 10.1080/15548627.2019.1659612

[37] Vézina C, Kudelski A, Sehgal SN. Rapamycin (AY-22,989), a new antifungal antibiotic. I. Taxonomy of the producing streptomycete and isolation of the active principle. *J Antibiot (Tokyo)*. 1975;28(10):721–726. doi: 10.7164/antibiotics.28.721

[38] Feng M, Kim J, Field K, Reid C, Chatzistamou I, Shim M. Aspirin ameliorates the long-term adverse effects of doxorubicin through suppression of cellular senescence. *FASEB Bioadv*. 2019;1(9):579–590. doi: 10.1096/fba.2019-00041

[39] Aljobaily N, Viereckl MJ, Hydock DS, *et al*. Creatine Alleviates Doxorubicin-Induced Liver Damage by Inhibiting Liver Fibrosis, Inflammation, Oxidative Stress, and Cellular Senescence. *Nutrients*. 2020;13(1):41. doi: 10.3390/nu13010041